Development of a polarized hyperspectral microscope for cardiac fiber orientation imaging

Zhou, Ximing, Dormer, James, Fei, Baowei

Ximing Zhou, James Dormer, Baowei Fei, "Development of a polarized hyperspectral microscope for cardiac fiber orientation imaging," Proc. SPIE 11215, Diagnostic and Therapeutic Applications of Light in Cardiology 2020, 112150V (25 February 2020); doi: 10.1117/12.2549720

SPIE.

Event: SPIE BiOS, 2020, San Francisco, California, United States

Development of a polarized hyperspectral microscope for cardiac fiber orientation imaging

Ximing Zhou [a], James Dormer [a] and Baowei Fei [a,b,*]

[a]The University of Texas at Dallas, Department of Bioengineering, Richardson, TX
[b]University of Texas Southwestern Medical Center, Department of Radiology, Dallas, TX

ABSTRACT

Myocardial fiber orientation is closely related to the functions of the heart. The development of imaging tools for depicting myocardial fiber orientation is important. We developed a polarized hyperspectral imaging microscope (PHSIM) for cardiac fiber orientation imaging, which is capable of polarimetric imaging and hyperspectral imaging. Polarimetric imaging is realized by the integration of two polarizers. Hyperspectral imaging is realized by snapscan Preliminary imaging experiments were implemented on an unstained paraffin embedded tissue slides of a chicken heart. We also set up a Monte Carlo simulation program based on the cylinder optical model to simulate the cardiac fiber structure of the sample and the optical setup of the PHSIM system, in which we can calculate the system output light intensity related to cardiac fiber orientation. According to the imaging and simulation results, there exists a variation of intensity of acquired images with the polar angles from the maximum to the minimum under different wavelengths, which should relate to the orientation of cardiac fibers. In addition, there is a shift of the polar angle where the maximum intensity appears when a rotation of the sample happened both in the simulation and imaging experiments. Further work is required for imaging more types of myocardial tissues at different parts and the design of a complete quantitative model to describe the relations among polar angles, wavelengths, and cardiac fiber orientations.

Keywords: Hyperspectral imaging, polarized light imaging, Stokes vector, cardiac fiber, Monte Carlo simulation.

1. INTRODUCTION

Myocardial fiber organization can significantly influence the functioning of heart because action potential can propagate up to 10 times faster along the longitudinal direction of myocardial fibers than along the transverse direction [1]. Several imaging techniques have been adopted for imaging cardiac fibers, such as histology [2, 3, 4], optical coherence tomography (OCT) [1, 5, 6, 7, 8, 9, 10, 11], second harmonic generation (SHG) microscopy [12, 13], polarized light imaging [14] and susceptibility weight imaging (SWI) [15]. Polarized light related optical imaging methods are promising in quantitative analysis of cardiac fiber orientation as is shown in the papers which applied polarization-sensitive optical coherence tomography (PS-OCT) [1, 5, 10, 11] or polarized light imaging. Among those optical imaging methods, SHG microscope is an effective tool for the evaluation of cardiac fiber orientation in the cardiac tissue slides. However, SHG is expensive and may be difficult to be applied for *in vivo* purposes due to low SHG signals.

This study aims at the development of a polarized hyperspectral imaging microscope (PHSIM) which combines hyperspectral imaging and polarized light imaging, adding the wavelength dimension to the polarized light imaging parameters. The system is developed for quantitative analysis of cardiac fiber orientation, and has the potential to become a high speed imaging system for the heart.

2. METHODS

2.1 System setup

The polarized hyperspectral microscope system consists of a visible and near infrared (VNIR) hyperspectral camera, two polarizers, and a transmission mode microscope, as is shown in Figure 1. The hyperspectral scanning method of the system

Diagnostic and Therapeutic Applications of Light in Cardiology 2020, edited by Kenton W. Gregory, Laura Marcu,
Proc. of SPIE Vol. 11215, 112150V · © 2020 SPIE · CCC code: 1605-7422/20/$21 · doi: 10.1117/12.2549720

is snapscan, in which the scanning is achieved by the movement of CCD detectors inside the camera rather than the movement of samples. The polarization state of light is modulated by rotating the polarizers during the snapscan scanning process. Finally, the complete dataset which contains hyperspectral information and polarized light information is obtained.

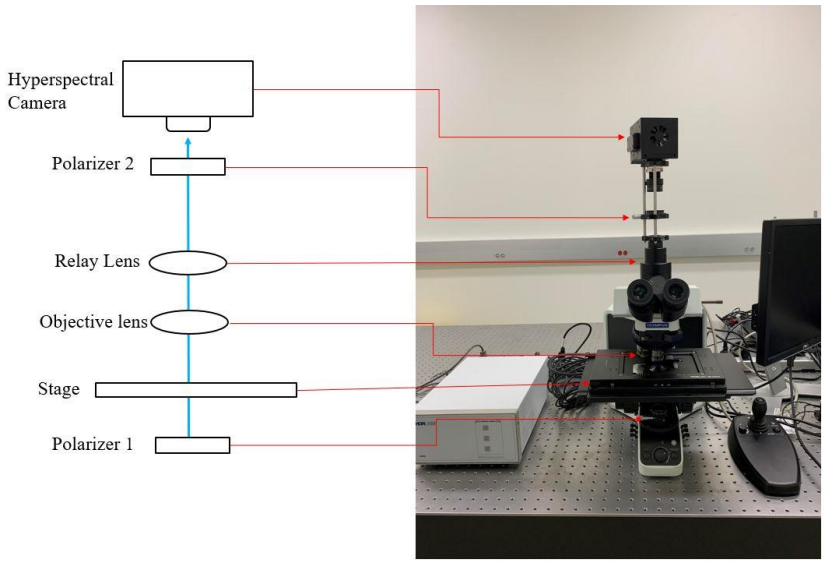

Fig 1. The setup of the polarized hyperspectral imaging microscope. Polarized light imaging is realized by the synchronized rotation of two polarizers, and hyperspectral imaging is realized by snapscan based on the hyperspectral camera.

2.2 Data acquisition and processing

The developed polarized hyperspectral microscope is capable of polarimetric imaging. In this study, we used a rotational polarimetric imaging method, in which the two polarizers in the system were synchronized at angles ranging from 0 to 180 degrees at an increment of 5 degrees. The hyperspectral data cube was acquired under each polar angle. Figure 2 demonstrates the flow chart of the data acquisition process. After the acquisition of images, we calculated the average intensity of the image at three wavelengths (486 nm, 552 nm, 700 nm) on a region of interest (ROI) of 100 ×100 pixels collected under the polar angles from 0 to 180 degrees. The whole process was repeated once after we rotated the sample for 30 degrees.

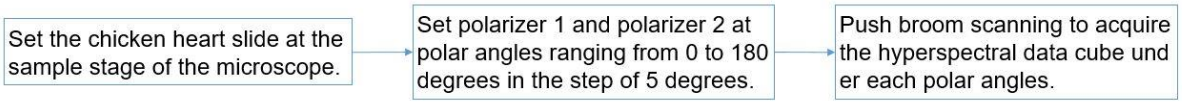

Fig 2. Flowchart of data acquisition process.

2.3 Sample preparation

One complete fresh healthy chicken heart was firstly processed in a fully enclosed tissue processor for 8 hours, then embedded in paraffin by a cold and hot paraffin embedding station. In the next step, four 20 μm unstained tissue slides were obtained by a manual microtome. One tissue slide was imaged under the polarized hyperspectral microscope by the rotational polarimetric imaging method described in the previous section.

2.4 Simulation

In this paper, a polarization imaging model was set up by us to study the properties of the light transmitted from cardiac fibers. The infinite long cylinders align in the x-z plane at α degrees with respect to x axis. Figure 3 is a schematic of the cardiac fiber model in the simulation program. We only detect the total light intensity. As the linear polarized incident light illuminates the fibers at normal incidence, the linearly polarized transmitted light is collected at the same polar angle. In other words, the illumination and the collection are co-polarized; thus, only the photons with the same polarization as the incident photons are collected. Furthermore, in the simulation experiments, we simulated the condition when the polar angle of the two polarizers changed from 0 to 180 degrees. At this moment, we only conducted the simulation under 550 nm, and the light intensity is calculated based on photon numbers. We referred to [16] in setting up the simulation program.

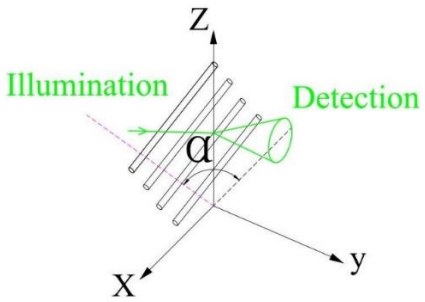

Fig 3. A schematic of the cardiac fiber model in the simulation program.

3. RESULTS

As mentioned in the data acquisition and processing part above, we obtained the hyperspectral data cube of the chicken heart slides under the polar angles between 0 to 180 degrees at steps of 10 degrees. Figure 4 demonstrates the synthetic RGB images based on three wavelengths (486 nm, 552 nm, 700 nm) of one slide at its original position and 30 degrees position, in which the polar angle was both set to 0 degrees and 100 degrees. Figure 5 plots the curves between the intensity of the images and the polar angles under the three wavelengths (486 nm, 552 nm, 700 nm). The results show that there is variation of intensity of acquired images with the polar angles from the maximum to the minimum under different wavelengths, and the intensity of the images under the same polar angle are different among the different wavelengths. In addition, when repeating the experiment after we rotated the sample orientation for 30 degrees counterclockwise, the maximum value of the curves shifted 30 degrees at the same time. The reason should possibly be that the polar angles of the scattering of cardiac fibers to the incident light is sensitive to its polar angles.

The simulation results are illustrated in Figure 6. We simulated the condition when the polar angle of the two polarizers changed from 0 to 180 degrees, and the sample orientation was set at three orientations (30 degrees, 90 degrees, 120 degrees). The simulation results and the imaging results shared the two similarities, including the variation of image intensities with the variation of polar angles, and the shift of the maximum value for the intensity curve with the rotation of sample orientations. The two-dimension simulation results are shown in pseudo-color image form, which demonstrate the image intensities of sample orientations at 30 degrees, 90 degrees, and 120 degrees when the polar angles of two polarizers are set at 0 degrees, and the wavelength was set at 550nm. The intensity curves were plotted based on the average intensity of pixels from simulation results.

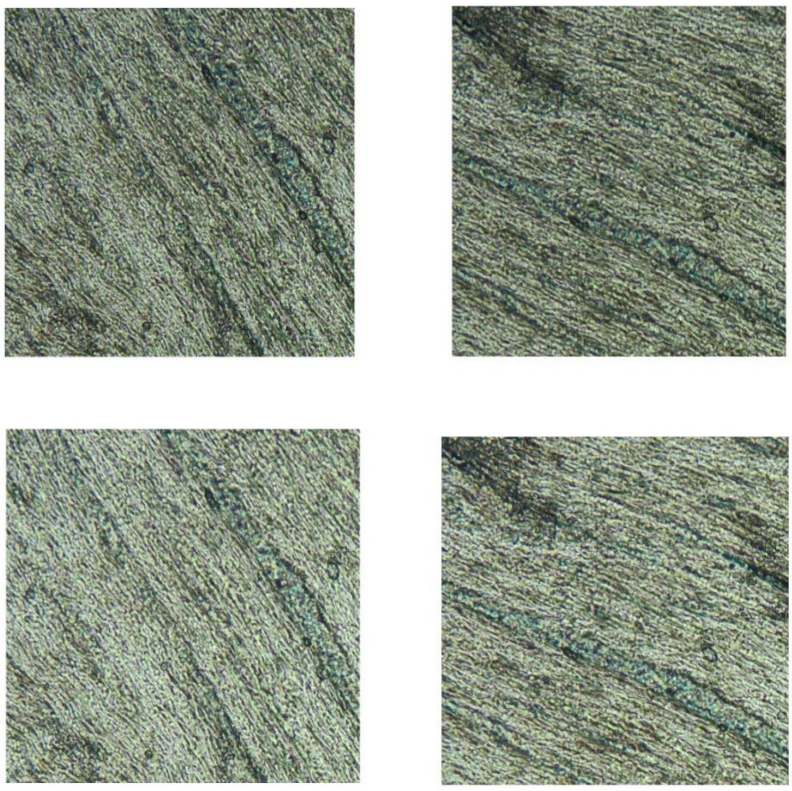

Figure 4. The synthetic RGB images of one slide at its original position and 30 degrees position, in which the polar angle was both set to 0 degrees at the first row of images, and set to 100 degrees at the second row of images.

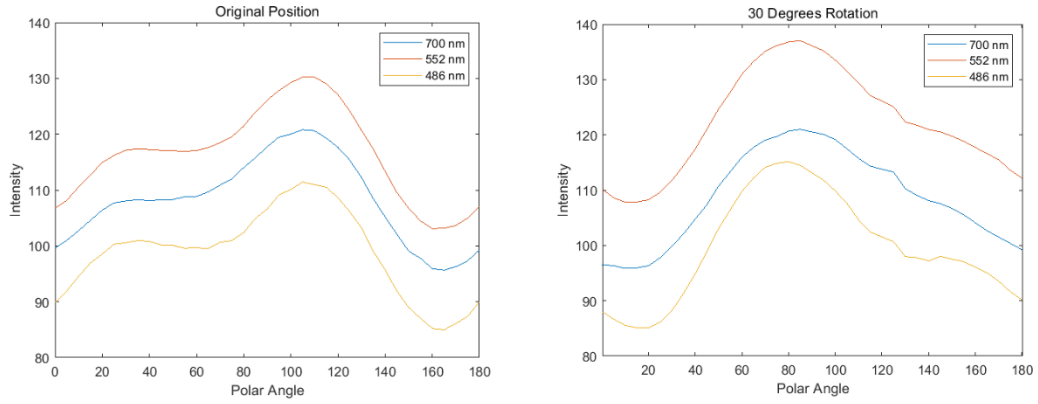

Figure 5. The curves for intensity of images under polar angles from 0 to 180 degrees at three wavelengths (486 nm, 552 nm, 700 nm) when the tissue slide is placed at its original orientation and rotated for 30 degrees.

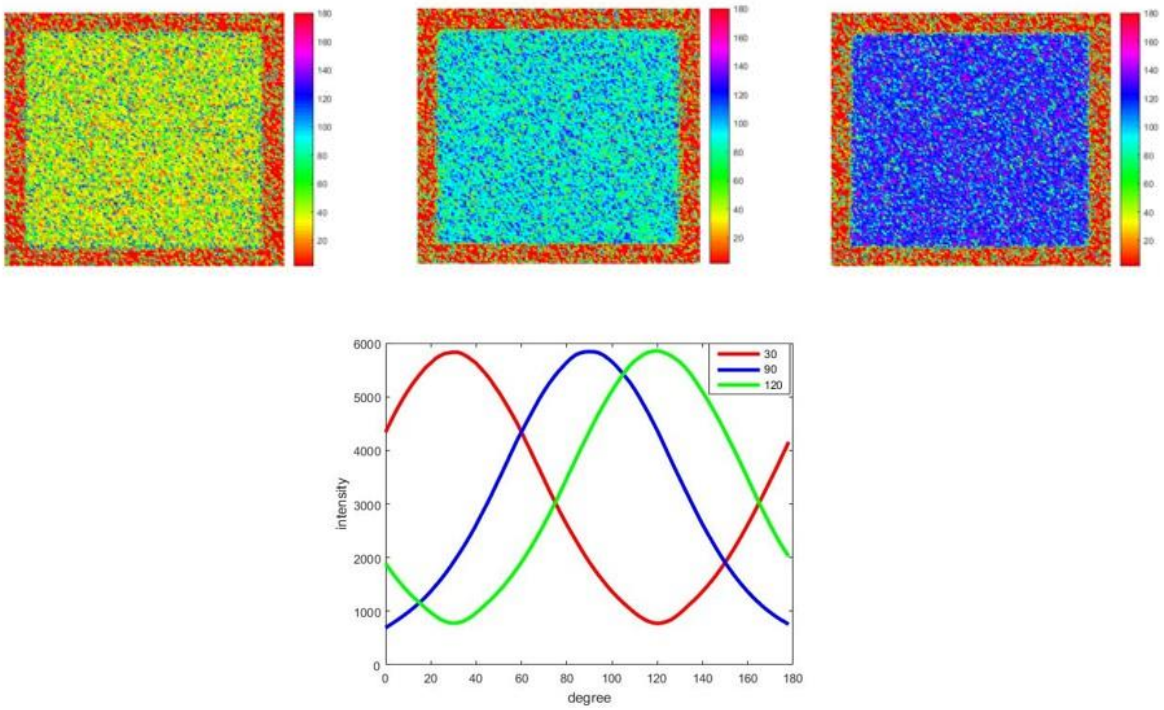

Figure 6. The results of Monte Carlo simulation. The three images on the first row are pseudo-color images of intensities for sample orientations at 30 degrees, 90 degrees, and 120 degrees, and the polar angle is 0 degree. The image on the second row shows the plots of intensities and polar angles (0-180 degrees) for the sample orientations at 30 degrees, 90 degrees, and 120 degrees.

4. CONCLUSIONS AND DISCUSSIONS

To the best of our knowledge, this is the first attempt to use polarized hyperspectral imaging rather than only polarized light imaging for the evaluation of cardiac fiber orientation, and conduct Monte Carlo simulation for comparison.

We developed a polarized hyperspectral imaging system based on snapscan and rotational polarimetric imaging. The preliminary results demonstrate that images acquired by the polarized hyperspectral microscope can depict the cardiac fiber orientation based on the synthetic RGB images from the hyperspectral data cube, and there is a variation of intensity of the acquired images with the switch polar angles from the maximum to the minimum under different wavelengths, which should relate to the orientation of cardiac fibers. Furthermore, there is a shift of the maximum intensity in the intensity curves when rotating the sample both in the simulation and imaging experiments. Future work is required for imaging more types of myocardial tissues at different parts and design a complete quantitative model to describe the relations among polar angles, wavelengths, and cardiac fiber orientations, with the assistance of numerical simulations.

ACKNOWLEDGEMENTS

The research was supported in part by the Cancer Prevention and Research Institute of Texas (CPRIT) grant RP190588.

REFERENCES

1. Wang, Y., et al. "Histology validation of mapping depth-resolved cardiac fiber orientation in fresh mouse heart using optical polarization tractography." *Biomedical optics express* 5.8 (2014): 2843-2855.
2. Scollan, David F., et al. "Histological validation of myocardial microstructure obtained from diffusion tensor magnetic resonance imaging." *American Journal of Physiology-Heart and Circulatory Physiology* 275.6 (1998): H2308-H2318.
3. Hsu, E. W., et al. "Magnetic resonance myocardial fiber-orientation mapping with direct histological correlation." *American Journal of Physiology-Heart and Circulatory Physiology* 274.5 (1998): H1627-H1634.
4. Karlon, William J., et al. "Automated measurement of myofiber disarray in transgenic mice with ventricular expression of ras." *The Anatomical Record: An Official Publication of the American Association of Anatomists* 252.4 (1998): 612-625.
5. Sun, Chia-Wei, et al. "Myocardial tissue characterization based on a polarization-sensitive optical coherence tomography system with an ultrashort pulsed laser." *Journal of biomedical optics* 11.5 (2006): 054016.
6. Fleming, Christine P., et al. "Quantification of cardiac fiber orientation using optical coherence tomography." *Journal of biomedical optics* 13.3 (2008): 030505.
7. Ashikaga, Hiroshi, et al. "Transmural dispersion of myofiber mechanics: implications for electrical heterogeneity in vivo." *Journal of the American College of Cardiology* 49.8 (2007): 909-916.
8. Gan, Yu, et al. "Automated classification of optical coherence tomography images of human atrial tissue." *Journal of biomedical optics* 21.10 (2016): 101407.
9. Ambrosi, Christina M., et al. "Quantification of fiber orientation in the canine atrial pacemaker complex using optical coherence tomography." *Journal of biomedical optics* 17.7 (2012): 071309.
10. Gan, Yu, and Christine P. Fleming. "Extracting three-dimensional orientation and tractography of myofibers using optical coherence tomography." *Biomedical optics express* 4.10 (2013): 2150-2165.
11. Wang, Y., et al. "Heart structural remodeling in a mouse model of Duchenne cardiomyopathy revealed using optical polarization tractography." *Biomedical optics express* 8.3 (2017): 1271-1276.
12. Chen, Szu-Yu, Chin-Ying Stephen Hsu, and Chi-Kuang Sun. "Epi-third and second harmonic generation microscopic imaging of abnormal enamel." *Optics express* 16.15 (2008): 11670-11679.
13. Sommer, Gerhard, et al. "Biomechanical properties and microstructure of human ventricular myocardium." *Acta biomaterialia* 24 (2015): 172-192.
14. Yang, Feng, et al. "Quantitative comparison of human myocardial fiber orientations derived from DTI and polarized light imaging." *Physics in Medicine & Biology* 63.21 (2018): 215003.
15. Lee, Wei-Ning, et al. "Mapping myocardial fiber orientation using echocardiography-based shear wave imaging." *IEEE transactions on medical imaging* 31.3 (2011): 554-562.
16. Yang, Bin, et al. "Polarized light spatial frequency domain imaging for non-destructive quantification of soft tissue fibrous structures." *Biomedical optics express* 6.4 (2015): 1520-1533.